



TITLE:

A comparison between Dc'-values obtained from a dynamic rupture model and waveform inversion

AUTHOR(S):

Yasuda, Takumi; Yagi, Yuji; Mikumo, Takeshi;
Miyatake, Takashi

CITATION:

Yasuda, Takumi ...[et al]. A comparison between Dc'-values obtained from a dynamic rupture model and waveform inversion. Geophysical Research Letters 2005, 32(4): L14316.

ISSUE DATE:

2005-07-28

URL:

<http://hdl.handle.net/2433/193415>

RIGHT:

Copyright 2005 by the American Geophysical Union.

A comparison between D_c' -values obtained from a dynamic rupture model and waveform inversion

Takumi Yasuda,¹ Yuji Yagi,² Takeshi Mikumo,³ and Takashi Miyatake¹

Received 4 April 2005; revised 10 June 2005; accepted 30 June 2005; published 29 July 2005.

[1] We investigate the validity of a method for estimating the critical slip-weakening distance (D_c), which was proposed by Mikumo and Yagi [2003], for a dynamic rupture model of a recent earthquake. Assuming a uniform distribution of D_c on the fault, we simulated spontaneous dynamic rupture process and generated the synthetic waveforms that would be observed at actual recording stations. Then, we carried out kinematic inversion of the synthetic waveforms and obtained the slip-rate time functions on each subfault. We estimate D_c from these functions and discuss whether the assumed D_c could be recovered correctly. We also investigated the rupture propagation effect over each subfault with a finite dimension and the effects from the waveform inversion and band-pass filtering processes on the estimate of D_c . We found that the propagation effect could cause an apparent correlation between the recovered D_c' -values and the final slip. **Citation:** Yasuda, T., Y. Yagi, T. Mikumo, and T. Miyatake (2005), A comparison between D_c' -values obtained from a dynamic rupture model and waveform inversion, *Geophys. Res. Lett.*, 32, L14316, doi:10.1029/2005GL023114.

1. Introduction

[2] Slip-weakening behavior of shear stress on earthquake faults plays a critical role in the dynamic part of the rupture process and hence on strong ground motions during large earthquakes. Accordingly, it is important in rupture dynamics to study the critical slip-weakening distance at which the shear stress drops to the frictional stress level. A number of seismologists have investigated the critical slip-weakening distance D_c by theoretical studies [e.g., Ida, 1972; Andrews, 1976a, 1976b; Matsu'ura *et al.*, 1992], from laboratory experiments [e.g., Okubo and Dieterich, 1984; Ohnaka, 2000] and based on seismic waveform observations [e.g., Ide and Takeo, 1997; Olsen *et al.*, 1997; Guatteri and Spudich, 2000].

[3] Recently, Mikumo *et al.* [2003] estimated the critical slip-weakening distance on earthquake faults, by applying a new approach. This approach is based on the finding that the breakdown time of shear stress T_b is well correlated with the time of peak slip-velocity T_{pv} at each point on the fault except at points near fault edges and strong barriers, and that D_c at time T_b may be approximately estimated from slip

D_c' at time T_{pv} . The validity of this approximation has been justified by Fukuyama *et al.* [2003] from theoretical considerations and numerical experiments. The above method has later been applied to several large earthquakes [Mikumo and Yagi, 2003; Zhang *et al.*, 2003; Miyatake *et al.*, 2004]. The estimated D_c values appear to be spatially variable and also proportional to the final slip. There is a possibility, however, that such proportionality might be an artifact due to low-pass filtering and/or smoothing effects of recorded waveforms during the inversion procedure [Spudich and Guatteri, 2004], and also due to the assumed shape of the source time function [Piatanesi *et al.*, 2004].

[4] The main purpose of the present study is to investigate the validity of the method proposed by Mikumo *et al.* [2003]. Firstly, we construct a hypothetical dynamic rupture model for an earthquake, with a uniform D_c distribution. As a second step, we generate the synthetic waveforms from this model for a number of recording stations. Then, we carry out kinematic inversion of the waveforms to obtain the mean slip rate time function on each subfault. Following Mikumo *et al.* [2003], we try to calculate D_c' from the mean slip rate time functions to see if the assigned D_c -value could be correctly recovered. We also investigate the effect from rupture propagation on subfaults, which has not been taken into consideration in the previous studies [e.g., Mikumo *et al.*, 2003], and the effects from waveform inversion and band-pass filtering on the estimate of D_c .

2. Dynamic Rupture Model

[5] In order to make an input data for waveform inversion in our simulation, we constructed a hypothetical dynamic rupture model for the 2001 Geiyo, Japan, earthquake ($M_w = 6.7$), with an assumption of uniform D_c distribution, by referring to the previous model proposed by Miyatake *et al.* [2004]. In the manuscript we use "dynamic model" for dynamic rupture computation in which elastodynamic equations of motion are solved with the dynamic (stress) boundary condition [Kostrov and Das, 1988, p. 49]. Following Miyatake *et al.* [2004], we assumed the fault dimension of 40km long and 25km wide. We also referred to the rupture time distribution estimated from the delay time of kinematic "mean slip rate" time function on the subfault, the final slip distribution and the static shear stress change distribution that have been obtained in the kinematic model of Miyatake *et al.* [2004]. Assuming that the dynamic behavior of shear stress change follows a simplified slip-weakening law [Andrews, 1976a, 1976b], we assumed a critical slip-weakening distance of 25 cm distributed uniformly over the fault instead of heterogeneous distribution of D_c [Miyatake *et al.*, 2004], because one of the purpose of

¹Earthquake Research Institute, University of Tokyo, Tokyo, Japan.

²Graduate School of Life and Environmental Sciences, University of Tsukuba, Tsukuba, Japan.

³Instituto de Geofísica, Universidad Nacional Autónoma de México, Ciudad Universitaria, México D.F., México.

		Strike direction																	
Dip direction	1	11	21	31	41	51	61	71	81	91	101	111	121	131	141	151			
	2	12	22	32	42	52	62	72	82	92	102	112	122	132	142	152			
	3	13	23	33	43	53	63	73	83	93	103	113	123	133	143	153			
	4	14	24	34	44	54	64	74	84	94	104	114	124	134	144	154			
	5	15	25	35	45	55	65	75	85	95	105	115	125	135	145	155			
	6	16	26	36	46	56	66	76	86	96	106	116	126	136	146	156			
	7	17	27	37	47	57	67	77	87	97	107	117	127	137	147	157			
	8	18	28	38	48	58	68	78	88	98	108	118	128	138	148	158			
	9	19	29	39	49	59	69	79	89	99	109	119	129	139	149	159			
	10	20	30	40	50	60	70	80	90	100	110	120	130	140	150	160			

Figure 1. Subfault index.

our study is to study whether the correlation between obtained D_c' and the final slip is artificial or not. Firstly, we solve the 3D elastodynamic equations imposing the fault boundary condition of slip-weakening law with fixed rupture times on the fault, by using the 4th-order finite difference method (FD) with 3D staggered grids, where the grid interval and the time increment are taken as 0.25 km and 0.005 s, respectively. This case is not exactly a spontaneous rupture model and may be called a “quasidynamic model”. At each time step in FD computations, the calculated stress just before the arrival of rupture front is considered to be the strength excess at each point on the fault. Given the distribution of strength excess, the uniform D_c distribution, heterogeneous stress drop and uniform initial stress, we performed spontaneous rupture simulations again by solving the elastodynamic equations, and then we calculated the slip D_c' (denoted by $D_c'^1$) at the time of peak of the ‘dynamically-generated’ slip rate time function on each of the grid points.

3. Waveform Inversion Analysis

[6] We generated the synthetic waveforms from point source summation of 160×100 dynamic slip rate time functions described before, for teleseismic P-waves at 15 stations and for 12 components of near-field P- and S-waves at 4 strong-motion stations, which have been used by Miyatake *et al.* [2004]. The Green’s functions for teleseismic P-waves were calculated by using Kikuchi and Kanamori’s [1991] method and those for near-field ground

motions were calculated by the discrete wave number method developed by Kohketsu [1985]. The structure model used to compute both the teleseismic body waves and near-source ground motions are shown by Miyatake *et al.* [2004, Table 1].

[7] In order to set the same situation as in the actual kinematic waveform inversion, the teleseismic synthetic waveforms and the near-source synthetic waveforms were bandpassed between 0.01 to 1.0 Hz and 0.1 to 0.5 Hz, respectively. We used a causal 4th-order Butterworth filter passed forward and backward to the time series.

[8] We then carried out inversion of the synthetic waveforms obtained from the above procedure. This waveform inversion was performed by the same method as described by Yagi *et al.* [2004]. In this case, the fault was divided into 16×10 subfaults (as indicated in Figure 1), each having an area of 2.5 km \times 2.5 km. Applying a multi-time window analysis [e.g., Yoshida, 1992], the slip rate time function on each subfault was expanded in a series of 32 overlapped triangle functions with a rise time of 0.15 s. To stabilize the solution, we imposed here a smoothness constraint on the time and space distribution of slip, using an optimized Akaike’s Bayesian information criterion (ABIC) [e.g., Yagi *et al.*, 2004]. From these procedures, we determined the slip distribution on the fault (Figure 2a). It should be noted that a single point source is used as the subfault Green’s function, and that rupture propagation is not included in the subfault Green’s function.

[9] In Figure 2b, the ‘inverted mean’ slip rate time functions indicated by red curves are compared with the ‘dynamically-generated mean’ slip rate time functions indicated by black curves that are the sum of the dynamic slip rate time functions within each subfault, summed at constant absolute time, which causes them to be broadened by the propagation of rupture within each subfault. It can be seen that the two time functions fit quite well each other. We calculate $D_c'^2$ distribution at the time of peak of the ‘dynamically generated mean’ slip rate time functions.

4. Result and Discussions

[10] We compare three different types of the slip rate time functions to calculate the slip amount D_c' , following the method proposed by Mikumo *et al.* [2003]. We calculated the slip $D_c'^1$ at the time of peak of the ‘dynamically-

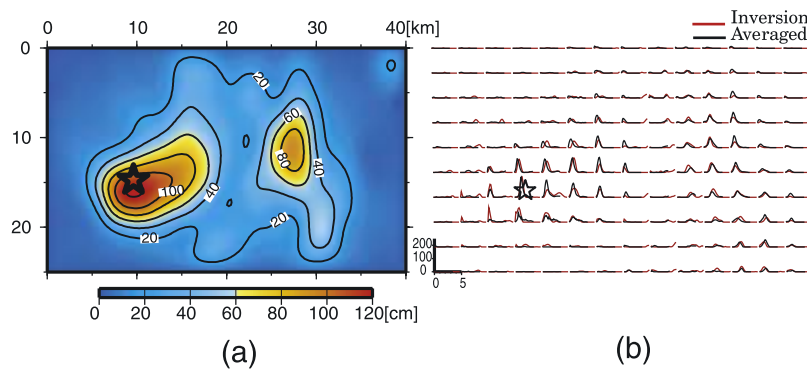


Figure 2. (a) Spatial distribution of final slip. (b) Slip-rate time functions on the subfaults. The star, red lines and black lines indicate the hypocenter, the functions derived from the inversion result and the functions derived from the dynamic model, respectively.

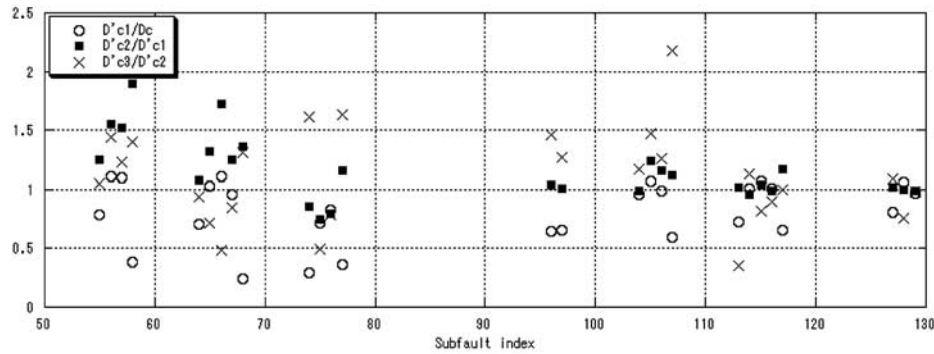


Figure 3. $D_c'^1/D_c$, $D_c'^2/D_c'^1$ and $D_c'^3/D_c'^2$ for selected subfaults.

generated' slip rate time function on each grid point, the slip $D_c'^2$ at the time of peak of the 'dynamically-generated mean' slip rate time function on each subfault, and the slip $D_c'^3$ at the time of peak of the 'inverted mean' slip rate time function on the corresponding subfault. It should be noted that the inverted slip rate time functions obtained by this waveform inversion are elongated to include the effect of rupture propagation inside the subfaults because our subfault is modeled as a point source.

[11] Following Mikumo's criterion, we exclude the data of the following locations; a) faults edges, b) barriers and its vicinity, c) final slip values smaller than 30 cm, d) the rupture starting area and its vicinity.

[12] $D_c'^1$ does not correspond exactly to D_c because of the time difference between T_b and T_{pv} [Mikumo *et al.*, 2003]. $D_c'^2$ -values differ slightly from $D_c'^1$ because of blurring effects of rupture propagation inside each larger subfault. $D_c'^3$ additionally includes the effect of the inversion. Using the above three D_c' s, we can discuss the following sources of contamination in estimating D_c ; (1) the difference between the break down time of stress drop and the time of peak of the slip rate (2) the effect of omission of rupture propagation inside the larger-size subfaults in parameterization of the inversion process and (3) the inversion process (except the source modeling) with band-pass filtering and a smoothness constraint. In order to study the above effects (1), (2) and (3), we calculate $D_c'^1/D_c$, $D_c'^2/D_c'^1$ and $D_c'^3/D_c'^2$ as shown in Figure 3 for selected subfaults after applying the above criterion. We also calculate the mean value and standard deviations of $D_c'^1/D_c$, $D_c'^2/D_c'^1$, $D_c'^3/D_c'^2$ (Table 1 and Figure 4) where we omitted the data for slip tentatively less than 30 cm or 60 cm.

Table 1. The Mean Value and Standard Deviations of $D_c'^1/D_c$, $D_c'^2/D_c'^1$ and $D_c'^3/D_c'^2$

	$D_c'^1/D_c$	$D_c'^2/D_c'^1$	$D_c'^3/D_c'^2$
D > 30 cm			
Data	32	32	32
Mean	0.76	1.17	1.13
Standard deviation	0.26	0.25	0.40
D > 60 cm			
Data	11	11	11
Mean	1.02	1.27	1.03
Standard deviation	0.09	0.24	0.30

[13] In Figures 3 and 4, $D_c'^1/D_c$ -values are somewhat smaller than 1, indicating that D_c' -values are partly consistent with the prescribed D_c or underestimated. $D_c'^2$ -values are almost consistent with $D_c'^1$ -values or overestimated on subfaults from No. 55 to No. 70. This comes from ignoring the effects of rupture propagation inside each subfault, which may correspond to a weighted average of the 10×10 slip rate time functions over each large-size subfault. This process is similar to the low-pass filtering effect which causes the elongation of D_c' [Spudich and Guatteri, 2004]. $D_c'^3$ -values seem to be scattered around $D_c'^2$ -values.

[14] All the $D_c'^1$, $D_c'^2$ and $D_c'^3$ values are plotted versus final slip in Figure 5. It seems that for slips less than 60 cm, $D_c'^1$ -values are scattered between 7 and 27 cm, (and might increase with slip), but almost constant for slips larger than 60 cm. $D_c'^2$ and $D_c'^3$ have an apparent proportionality with the final slip. It seems that $D_c'^3$ is about half the total slip, which agrees with the prediction of Spudich and Guatteri [2004] based on the central limit theorem. Considering that short slip causes poor resolution of D_c and that $D_c'^3$ includes

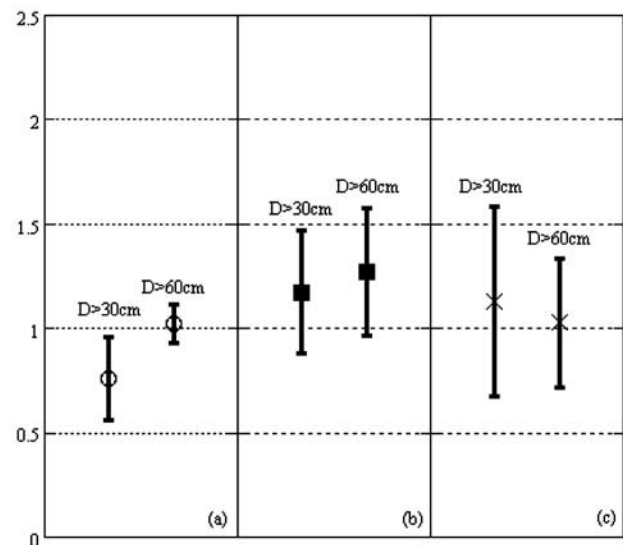


Figure 4. We also estimate the mean value and standard deviations of (a) $D_c'^1/D_c$, (b) $D_c'^2/D_c'^1$, (c) $D_c'^3/D_c'^2$ where we omitted the data of short slip less than 30 cm or tentatively 60 cm.

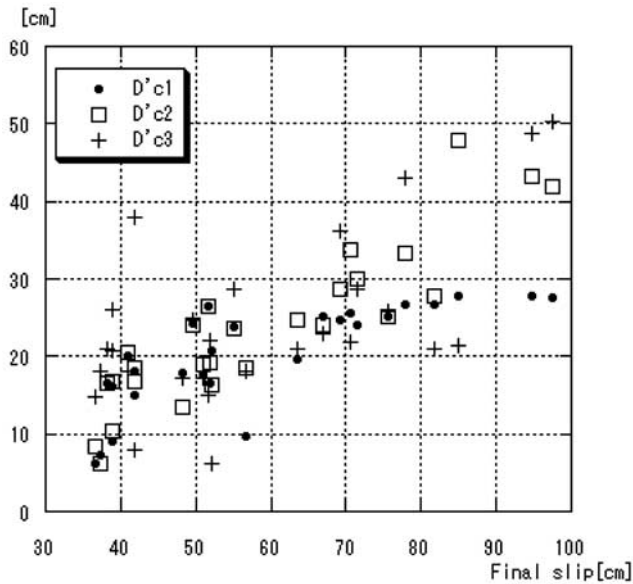


Figure 5. The estimated D_c' -values plotted versus the final slip on subfaults.

the above three effects, we conclude that the effects of rupture propagation inside the larger-size subfaults causes such an apparent correlation. *Spudich and Guatteri* [2004] mentioned that low-pass filtering causes an artificial correlation between D_c' and the final slip. Our calculations in this study show similar effects to their results. In our simulation, the effect of inversion with band-pass filter and smoothness constraint did not give a bias of D_c estimates, because the filtering effect is already included in $D_c'^2$. The averaged or low-pass-filtered slip rate time functions were not much changed by additional low-pass filtering during the inversion process.

5. Conclusions

[15] We have investigated the validity of the D_c estimation method, using a dynamic rupture model of the 2001 Geiyo earthquake. Following *Mikumo et al.* [2003], we estimated the critical slip-weakening distance and investigated whether the assumed value could be recovered correctly. We investigated the effect of rupture propagation on the larger-size subfaults adopted in the inversion process, which has not been taken into consideration in the previous studies [e.g., *Mikumo et al.*, 2003], and also studied the effects of the waveform inversion and band-pass filtering. We found that $D_c'^2$ calculated from the 'dynamically generated mean' slip rate functions deviates, to some extent, from the assumed value of 25 cm, and also that the rupture propagation effects inside the subfaults causes an apparent correlation between D_c and final slip. $D_c'^3$ obtained from the waveform inversion are relatively consistent with $D_c'^2$. As mentioned by *Spudich and Guatteri* [2004] and *Guatteri and Spudich* [2000], the effect of D_c on the waveforms in high frequency range seems to be quite large. If this information were retained in the inversion process, and if we could refine our method of estimation, it would not be

impossible to correct the obtained D_c' -values for the estimate of D_c distribution on the fault.

[16] **Acknowledgment.** We wish to thank Prof. Raul Madariaga and Dr. Paul Spudich for helpful comments.

References

- Andrews, D. J. (1976a), Rupture propagation with finite stress in antiplane strain, *J. Geophys. Res.*, **81**, 3575–3582.
- Andrews, D. J. (1976b), Rupture velocity of plane strain shear cracks, *J. Geophys. Res.*, **81**, 5678–5679.
- Fukuyama, E., T. Mikumo, and K. B. Olsen (2003), Estimation of the critical slip-weakening distance: Theoretical background, *Bull. Seismol. Soc. Am.*, **93**, 1835–1840.
- Guatteri, M., and P. Spudich (2000), What can strong-motion data tell us about slip-weakening fault friction laws?, *Bull. Seismol. Soc. Am.*, **90**, 98–116.
- Ida, Y. (1972), Cohesive force across the tip of a longitudinal-shear crack and Griffith's specific surface energy, *J. Geophys. Res.*, **77**, 3796–3805.
- Ide, S., and M. Takeo (1997), Determination of constitutive relations of fault slip based on seismic wave analysis, *J. Geophys. Res.*, **102**, 27,379–27,391.
- Kikuchi, M., and H. Kanamori (1991), Inversion of complex body waves- β , *Bull. Seismol. Soc. Am.*, **81**, 2335–2350.
- Koketsu, K. (1985), The extended reflectivity method for synthetic near-field seismograms, *J. Phys. Earth*, **33**, 121–131.
- Kostrov, B. V., and S. Das (1988), *Principles of Earthquake Source Mechanics*, Cambridge Univ. Press, New York.
- Matsu'ura, M., H. Kataoka, and B. Shibasaki (1992), Slip-dependent friction law and nucleation processes in earthquake rupture, *Tectonophysics*, **211**, 135–148.
- Mikumo, T., and Y. Yagi (2003), Slip-weakening distance in dynamic rupture of in-slab normal-faulting earthquakes, *Geophys. J. Int.*, **155**, 443–455.
- Mikumo, T., K. B. Olsen, E. Fukuyama, and Y. Yagi (2003), Stress-breakdown time and slip-weakening distance inferred from slip-velocity functions on earthquake faults, *Bull. Seismol. Soc. Am.*, **93**, 264–282.
- Miyatake, T., Y. Yagi, and T. Yasuda (2004), The dynamic rupture process of the 2001 Geiyo, Japan, earthquake, *Geophys. Res. Lett.*, **31**, L12612, doi:10.1029/2004GL019721.
- Ohnaka, M. (2000), A physical scaling relation between the size of an earthquake and its nucleation zone size, *Pure Appl. Geophys.*, **157**, 197–220.
- Okubo, P. G., and J. H. Dieterich (1984), Effects of physics fault properties on frictional instabilities produced on simulated faults, *J. Geophys. Res.*, **89**, 5817–5827.
- Olsen, K. B., R. Madariaga, and R. J. Archuleta (1997), Three-dimensional dynamic simulation of the 1992 Landers earthquake, *Science*, **278**, 834–838.
- Piatanesi, A., E. Tinti, M. Cocco, and E. Fukuyama (2004), The dependence of traction evolution on the earthquake source time function adopted in kinematic rupture models, *Geophys. Res. Lett.*, **31**, L04609, doi:10.1029/2003GL019225.
- Spudich, P., and M. Guatteri (2004), The effect of bandwidth limitations on the inference of earthquake slip-weakening distance from seismograms, *Bull. Seismol. Soc. Am.*, **94**, 2028–2036.
- Yagi, Y., T. Mikumo, J. Pacheco, and G. Reyes (2004), Source rupture process of the Tecoman, Colima, Mexico earthquake of January 22, 2003, determined by joint inversion of teleseismic body wave and near-field data, *Bull. Seismol. Soc. Am.*, **94**, 1795–1807.
- Yoshida, S. (1992), Waveform inversion for rupture process using a non-flat seafloor model: Application to 1986 Andreanof Islands and 1985 Chile earthquakes, *Tectonophysics*, **211**, 45–59.
- Zhang, W., T. Iwata, K. Irikura, H. Sekiguchi, and M. Bouchon (2003), Heterogeneous distribution of the dynamic source parameters of the 1999 Chi-Chi, Taiwan, earthquake, *J. Geophys. Res.*, **108**(B5), 2232, doi:10.1029/2002JB001889.

T. Miyatake and T. Yasuda, Earthquake Research Institute, University of Tokyo, Tokyo 113-0032, Japan. (tyasuda@eri.u-tokyo.ac.jp)

T. Mikumo, Instituto de Geofísica, Universidad Nacional Autónoma de México, Ciudad Universitaria, México 04510 D.F., México.

Y. Yagi, Graduate School of Life and Environmental Sciences, University of Tsukuba, Tsukuba 3050802, Japan.